Proceedings of the ASME 2014 International Design Engineering Technical Conferences & Computers and Information in Engineering Conference
IDETC/CIE 2014
August 17-20, 2014, Buffalo, New York, USA

DETC2014/VIB-35655

EXPLORING EQUILIBRIA IN STOCHASTIC DELAY DIFFERENTIAL EQUATIONS USING PERSISTENT HOMOLOGY

Firas A. Khasawneh *
Mechanical Engineering
State University of New York Institute of Technology
Utica, NY 13503
firas.khasawneh@sunyit.edu

Elizabeth Munch
Institute for Mathematics and its Applications
University of Minnesota
Minneapolis, Minnesota 55455
liz@ima.umn.edu

ABSTRACT

This paper explores the possibility of using techniques from topological data analysis for studying datasets generated from dynamical systems described by stochastic delay equations. The dataset is generated using Euler-Maryuama simulation for two first order systems with stochastic parameters drawn from a normal distribution. The first system contains additive noise whereas the second one contains parametric or multiplicative noise. Using Taken's embedding, the dataset is converted into a point cloud in a high-dimensional space. Persistent homology is then employed to analyze the structure of the point cloud in order to study equilibria and periodic solutions of the underlying system. Our results show that the persistent homology successfully differentiates between different types of equilibria. Therefore, we believe this approach will prove useful for automatic data analysis of vibration measurements. For example, our approach can be used in machining processes for chatter detection and prevention.

INTRODUCTION

Deterministic models for dynamical systems have been the subject of extensive research which has provided solutions for a wide range of initial conditions and different applied forces. Recently, there has been an increasing interest in random or stochastic systems. In contrast to deterministic systems, the state of a stochastic system cannot be determined exactly at any point in time. However, the likelihood that a future state will assume a certain value is described by statistical probabilities. In practice, all physical systems contain inherent nonlinearities and uncertainties and they operate in a noisy environment. Therefore, stochastic models are more capable of faithfully representing the real behavior of physical systems.

However, stochastic equations are infinite dimensional and analysis tools from deterministic models are not readily applicable to them. The analysis is more challenging if the dynamics involve delays and the system model is a stochastic delay differential equation (SDDE). These equations arise in many applications such as chemical kinetics [1], genetic networks [2], and machining processes [3, 4]. For a limited number of SDDEs, stochastic calculus can be used to study the stability of the first and second moments [5]. If the delay is small, then the SDDE can be approximated using a stochastic differential equation without the delay term [6]. An extension of the semi-discretization method for studying the moment stability of linear SDDEs with delays appearing in the drift term only was described in Ref. [7]. Another method to investigate the stability of this class of equations uses Lyapunov approach [8]. However, for the general case of SDDEs numerical simulation remains the most viable method of analysis.

Euler-Maryuama and Milstein simulation methods were extended to stochastic differential equations in [9–12] and [13], respectively. Numerical simulation provides a tool for generating path-wise solutions that can be easier to investigate than the original SDDE. For example, instead of directly studying the mean

*Address all correspondence to this author.

square (or more generally, the p^{th} mean) stability of the SDDE, which might be difficult or impossible, the paths generated by numerical simulation can be used [14–16]. The result of the numerical simulation is a time series or dataset that contains information about the system dynamics. Developing data analysis tools for these datasets has two benefits: 1) it provides a benchmark for testing new methods for the analysis of SDDE, and 2) the same tools can be used to analyze data from real-world applications.

Some of the data analysis methods for non-delayed stochastic equations include principal component analysis [17, 18], multi-dimensional scaling [19], local linear embedding [20], Laplacian eigenmaps [21], Hessian eigenmaps [22], local tangent space alignment [23], and diffusion maps [24–26]. The first step in many of these methods is to obtain a lower-dimensional representation of the underlying high-dimensional manifold. The hope is that the simplified representation captures the main features of the underlying dynamics. One of the key assumptions in many of the prominent data analysis methods for dynamical systems, e.g., diffusion maps, is that the underlying dynamics is Markovian. This precludes them from being used to study SDDEs which are non-Markovian.

In this paper we explore data analysis tools for datasets derived from SDDEs using topological data analysis. These tools are applicable to datasets arising from both experiments as well as simulations of dynamical systems. Specifically, we will use persistent homology to automatically detect when changes in the system behavior occur. In contrast to other data analysis tools, persistent homology does not require the system to be Markovian and it does not attempt to obtain a lower dimensional representation of a data set, but rather a low-dimensional descriptor which is easy to understand and which can be used to find quantities of interest.

We demonstrate the main concepts using a scalar stochastic delay equation that was used in Ref. [27]. The cases of both additive and multiplicative noise are investigated. In particular, we study the model SDDE in a region of the parameter space where noise can lead to sustained oscillations whereas a noise-free model predicts damped response, a phenomenon called coherence or stochastic resonance [27–33]. We use Euler-Maruyama method to simulate the SDDE within the deterministic stable region but near the stability boundary. We show that as the value of the delay is varied persistent homology can be used to detect the change of the response from a steady state equilibrium to a periodic orbit.

PERSISTENT HOMOLOGY

Persistent homology is a powerful tool arising in the context of Topological Data Analysis (TDA). It has found success in applications to many diverse fields such as neuroscience [34], medicine [35], sensor networks [36,37], and image analysis [38].

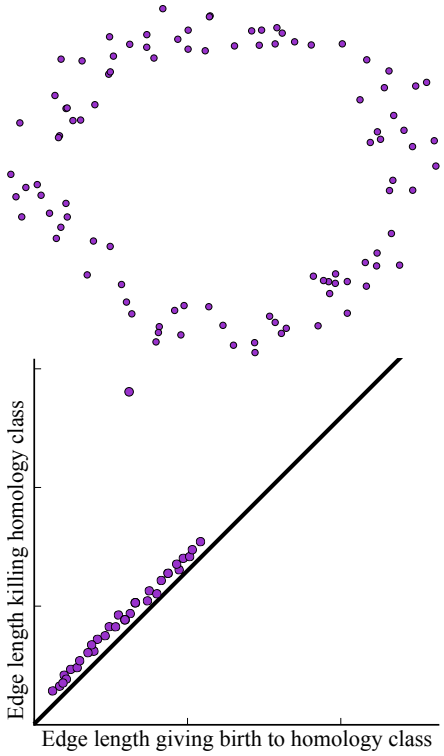

FIGURE 1. A point cloud and its persistence diagram. The circular structure of the point cloud is reflected in the single point far from the diagonal in the persistence diagram. The distance from this point to the diagonal can be used to quantify the circular structure.

We begin with an informal introduction to the subject, and direct the reader to [39, 40] for a full introduction to classical homology and to [41] for an introduction to persistence. Suppose we are given a point cloud drawn from a manifold and want to understand something about the underlying structure of the manifold. To do this we consider expanding discs centered at each point. We can then study the structure of the union of these discs for a changing radius. In the example of Fig. 1, we see that at a very small radius, we have merely a set of disconnected components. At a slightly larger radius, these discs start to intersect, possibly forming small circular structures which fill in at a slightly larger radius. What is very interesting is that at a relatively small radius, we form a circular structure around the full shape, but this takes a much longer time before it fills in.

In particular, given a set of points $\chi \subset \mathbb{R}^n$, we approximate the structure of the union of discs by a Rips complex, $\mathscr{R}_r$. This is a simplicial complex which consists of a vertex v_i associated to each point $x_i \in \chi$, and has an edge (v_i, v_j) any time the corresponding points are within distance r of each other, $\|x_i - x_j\| \leq r$. Then higher dimensional simplices are added whenever possible; that is, the simplex σ is in $\mathscr{R}_r$ iff $\|x_i - x_j\| \leq r$ for all $v_i, v_j \in \sigma$. Notice that since $\mathscr{R}_r \subset \mathscr{R}_s$ for $r < s$, we have a filtration $\{\mathscr{R}_r\}_{r>0}$.

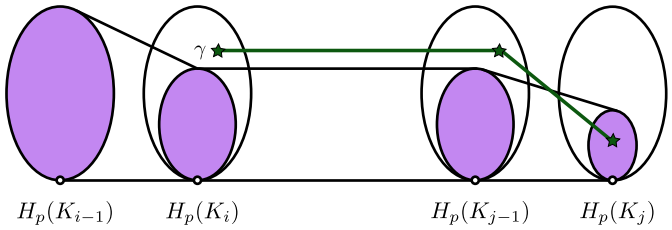

FIGURE 2. A schematic for understanding the birth and death of a persistent homology class. Classes are born if they do not appear in the image of the previous homology group under the maps induced by the filtration, and die when they merge with this image.

Let $H_p(\mathscr{R}_r)$ be the p-dimensional homology with $\mathbb{Z}_2$ coefficients. The inclusion $f : \mathscr{R}_r \hookrightarrow \mathscr{R}_s$ induces a map on homology, $f_*^{r,s} : H_p(\mathscr{R}_r) \to H_p(\mathscr{R}_s)$. A value r is called a homological critical value if for all sufficiently small $\delta > 0$, $f_*^{r-\delta,r} : H_p(\mathscr{R}_{r-\delta}) \to H_p(\mathscr{R}_r)$ is an isomorphism. Because we are interested in a finite point cloud χ, there are finitely many homological critical values, call them $r_1, \cdots, r_n$. Note that these radii are a subset of the set of pairwise distances between the points. For simplicity, we will replace $\mathscr{R}_{r_i}$ with K_i and $f_*^{r_i,r_j}$ with $f_*^{i,j}$.

A class γ is said to be born at r_i if $\gamma \in H_p(K_i)$ and it is not in the image of $f_*^{i-1,i} : H_p(K_{i-1}) \to H_p(K_i)$. This same class dies at r_j if it merges with the image of $H_p(K_{i-1})$ when entering $H_p(K_j)$; that is, if $f_*^{i,j-1}(\gamma)$ is not in $f_*^{i-1,j-1}(H_p(K_{i-1}))$ but $f_*^{i,j}(\gamma)$ is in $f_*^{i-1,j}(H_p(K_{i-1}))$. The persistence of the class is its lifetime, $r_j - r_i$. See Fig. 2.

To visualize this information, each class γ which is born at r_i and dies at r_j has a point drawn at (r_i, r_j) in what is called a persistence diagram. Classes which have small persistence show up as points close to the diagonal; classes which have large persistence appear as points far from the diagonal. In this way, we have a visual representation of the difference between classes which live a long time and which could be considered important, and the points representing short lived classes and which are often assumed to be noise.

Since its introduction in 2000 [42], persistence has found many applications. Most recently, a great deal of work has looked at using persistence for signal analysis [43, 44]. The idea behind Sliding Window 1-dimensional Persistent Homology, or Sw1Pers, is to use the Takens embedding, also known as the sliding window embedding, to turn a signal $X(t)$ into a point cloud in high dimensional space. Given a signal $X(t)$ along with a fixed η and D, we look at the set of points

$$SW_{D,\eta}X(t) = [X(t), X(t+\eta), \cdots, X(t+(D-1)\eta)] \in \mathbb{R}^D$$

for a fixed set of t. WLOG, we assume that X is defined on the interval $[0,T]$ and let L be the frequency of X. In [43], it was shown that the point cloud is roundest when the window size $D\eta$ is proportional to L. Periodicity in the signal translates into a point cloud with a circular structure. Since the first homology group gives information about loops, persistent homology is particularly good at finding and quantifying circular structure in point clouds. Thus, the periodicity of the signal can be studied by persistence diagram of the sliding window embedding. In particular, since we are looking for circular structure, we are interested in the furthest off-diagonal point in the 1-dimensional persistence diagram.

In order to study a particular signal, we fix a D which represents the dimension in which we will embed the point cloud, $\mathbb{R}^D$. A choice of D which is too low means that the structure of the embedding will not accurately reflect the dynamics; a high choice of D increases computation time due to the curse of dimensionality. Thus, we choose a relatively high dimension, $D = 15$, in order to be confident in our embedding, despite slowing down the computation. In the future, we will look for better methods for the dimension choice.

Let L be the number of windows of equal width which fit into $[0,T]$ or the frequency of the signal which we hope to see Then for a varying L, we set $D\eta$ to be the width of the sliding window for $\eta = \frac{T}{LD}$. See Fig. 4 for the relationship between L, D, η, and T. We then can compute the persistence diagram for each point cloud coming from each choice of L and look at the values for the persistence of the furthest off-diagonal point. If this point has a high persistence, the point cloud has a circular structure and thus the signal has a periodic structure. If we want to look the periodic structure for one particular signal, we can then look at the average of these values for all choices of L.

Unlike [43], we do not mean-shift and center the point cloud so that the farthest off-diagonal point has persistence in $[0,1]$. The technique was employed in the context of the original paper in order to compare the "periodic-ness" without considering other aspects of the signals. We do not do this because it does not differentiate between signals with different amplitudes like those that arise in our simulations.

MATHEMATICAL MODEL

We illustrate our results using a linear SDDE. Noise is introduced through additive and multiplicative terms, respectively, according to

$$dx = (\alpha x(t) + \beta x(t-\tau))dt + \delta dw, \tag{1a}$$
$$dx = (\alpha x(t) + \beta x(t-\tau))dt + \delta x(t) dw, \tag{1b}$$

where τ is a constant delay, α, β are constants, δ is a parameter that represents the noise intensity, and w is a standard Brownian motion. This equation was used to illustrate stochastic resonance in [27]. In the deterministic case, i.e., $\delta = 0$, the stability of

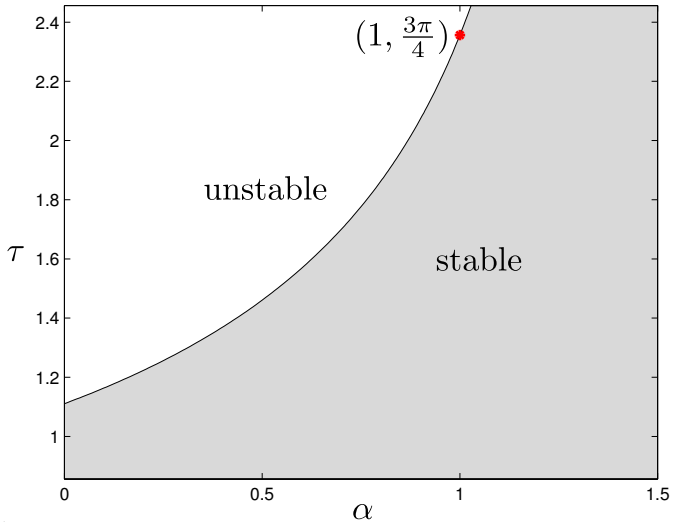

FIGURE 3. Stability diagram corresponding to Eq. (1a) with $\beta = -\sqrt{2}$. The point corresponding to the critical value of the delay for $\alpha = 1$ is also marked.

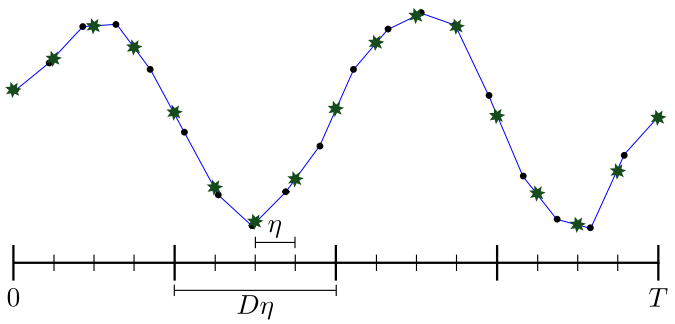

FIGURE 4. A schematic showing how the point cloud is generated. The simulated values for the signal are represented by the circles. D is fixed in advance. We split the domain $[0,T]$ into L regions of equal width. We determine η so that each region is $D\eta$. We then interpolate to approximate functions values at all multiples of η. Then we add a point to the point cloud in $\mathbb{R}^D$ by creating a vector of length D starting at each multiple of τ.

the equation in the (α,τ) parameter space and for $\beta = -\sqrt{2}$ is shown in Fig. 3. For $\alpha = 1$, the critical value for the delay at the stability boundary is $\tau_c = 3\pi/4$. It was shown in [27] that in the stable region near the point $(1,3\pi/4)$ the system follows a steady state equilibrium. If the stability boundary is crossed at $\tau_c = 3\pi/4$, the system demonstrates periodic oscillatory behavior. Including noise in the model triggers stochastic resonance where the system behavior becomes oscillatory for values of τ near the boundary but still within the stable region for the deterministic system.

NUMERICAL SIMULATION

Equations (1a) and (1b) were simulated using the Euler-Maryuama method described in [9] to generate the necessary datasets. The datasets were generated for points that lie along the line $\alpha = 1$ in the parameter space near $\tau_c = 3\pi/4$. The value of the delay was described by $\tau = \tau_c - \varepsilon$ where for higher values of ε we move away from the (deterministic) stability boundary towards the stable region while lower ε values push the system closer to the boundary. The range $\varepsilon \in [0.05, 1.5]$ was considered in this study. The time step used for the Brownian Path was $\delta t = 2^{-11}$, and the time step used in the Euler-Maruyama simulation was $\Delta t = 2^{-8}$. Since τ_c is irrational, the delay term requires intermediate values of x that lie between any two Brownian increments. In this case, we picked the value of x at the left end of the increment, similar to the procedure used in [7]. Because the time increments chosen were small, this approximation seems reasonable.

The Brownian path was created using Matlab and the approach described in [45]. For each set of simulation parameters, twenty datasets were generated and averaged. For each dataset, Matlab's command *rng('shuffle')* was used to seed the random number generator in order to produce a different path in each run. The history functions used over the interval $[-\tau, 0]$ for the additive and multiplicative noise cases were $x = 0.1$, and $x = 0.25\cos\left(\sqrt{\beta^2 - \alpha^2}\right)t$, respectively.

PERSISTENCE COMPUTATION

We next applied the Sw1Pers methodology to analyze the generated simulations. First, for each simulation $x_\varepsilon(t)$, we limited the domain of interest to $t \in [300, 400]$. The dimension D of Euclidean space in which to embed the point cloud was chosen to be 15. We define the parameter η to be the amount the window will be slid to obtain a new point for the point cloud as well as the distance between subsequent function values used to generate the point cloud. We then want to split the domain $[300, 400]$ into L windows of equal width $D\eta$ for different choices of L. Then for each $L \in \{1, 2, \cdots, 20\}$, $\eta = \frac{100}{LD}$. See Fig. 4 for a representation of the relationship between $T = 100$, D, L and η. We then used interpolation via python's *interpolate.splrep* command to determine the points

$$SW_{D,\tau}x_\varepsilon(t) = [x_\varepsilon(t), x_\varepsilon(t+\eta), \cdots, x_\varepsilon(t+D\eta)]$$

for $t = n\tau \in [300, 400 - D\eta]$, $n \in \mathbb{Z}$. Persistence was computed on this point cloud using the M12 package [46]. The persistence of the farthest off-diagonal point in the generated diagrams is plotted in the left column of Figs. 5 and 6. The average value for the maximum persistence for each ε is plotted in the right column of these figures.

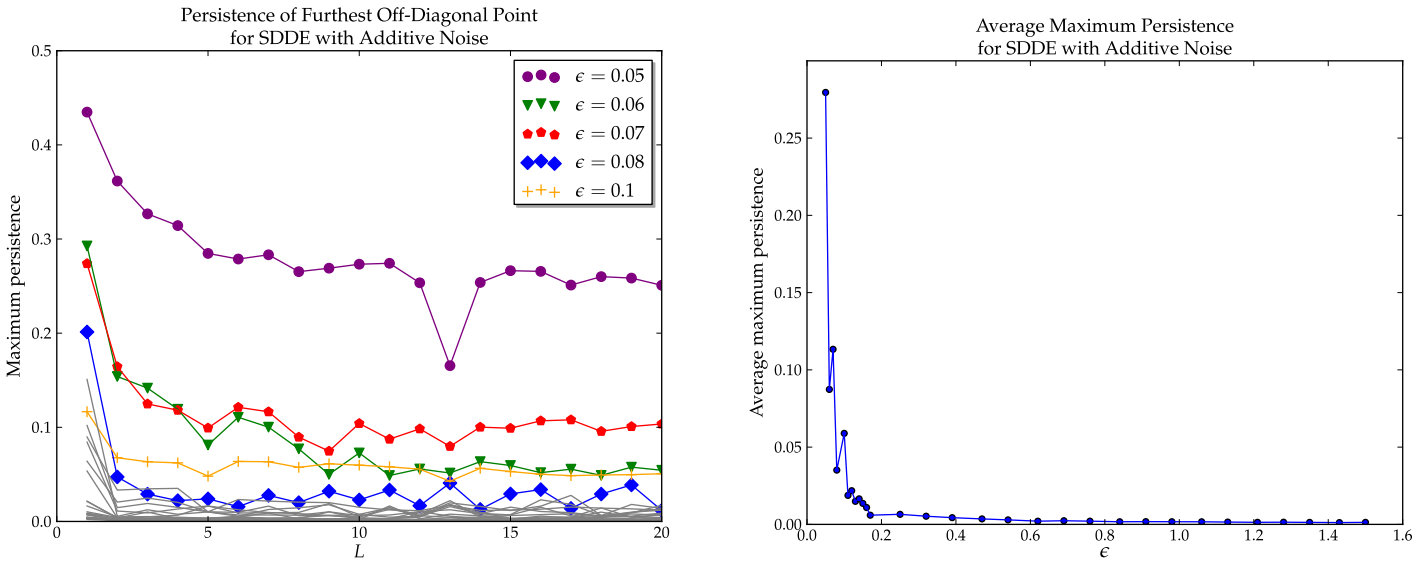

FIGURE 5. Results of analysis of data from simulations using additive noise. Using the sliding window embedding for varying choice of L, we compute the persistence diagram and mark the persistence of the furthest off-diagonal point in the graph at left. Several ε values are marked, while the lines for $\varepsilon > 0.1$ are drawn in gray. The average function value for each ε is drawn in the graph at right.

RESULTS AND CONCLUSIONS

For the case of additive noise described by Eq. (1a), the left column in Fig. 5 shows that for large values of ε, which correspond the points in the state space well below the deterministic instability boundary (see Fig. 3), the persistence diagram captured the steady state, non-oscillatory behavior of the system. This is shown by the gray lines which have maximum persistence very close to zero. However, as the value of ε is decreased, thus bringing the system closer to the instability boundary, we notice an increase in the maximum persistence followed by a jump at about $\varepsilon = 0.1$, which indicates that an oscillatory behavior has been detected. This is in agreement with the results reported in Ref. [27]. The right column of Fig. 5 averages the maximum persistence for each ε over all the corresponding values for L. This figure clearly shows how the oscillatory behavior disappears as the value of ε is decreased. One interesting observation is the drop in the maximum persistence at $L = 13$ for $\varepsilon = 0.05$ which deviates from an otherwise asymptotic behavior. In fact, this drop showed up in the maximum persistence diagrams for both additive and multiplicative noise at the same combination of $(L, \varepsilon) = (13, 0.05)$, see the left column of Fig. 6. One explanation for this behavior is that at this parameter combination the error due to dividing the data into the different sliding windows is maximized. However, further study is necessary to completely explain this behavior as well as the drop observed for $\varepsilon = 0.06$ and 0.08 in the corresponding average maximum persistence diagram for the additive noise case.

Figure 6 shows the maximum persistence (left column) and the average maximum persistence (right column) for the case of multiplicative noise described by Eq. (1b). The first row corresponds to noise intensity $\delta = 0.03$ while the second row corresponds to $\delta = 0.1$. Similar to the additive noise case in Fig (5), we see how persistent homology successfully captures the change in the system behavior from steady state equilibria to periodic oscillations as ε is decreased, thus causing τ to approach the deterministic instability boundary at τ_c. This is characterized by the increasing value of the maximum persistence as ε is decreased. Although Fig. 6 shows the same maximum persistence drop observed in Fig. 5 for $L = 13$ and $\varepsilon = 0.05$, the corresponding average maximum persistence diagrams do not contain the two kinks that appeared at $\varepsilon = 0.06$ and 0.08 in Fig. 5.

The results of this study show that persistent homology can be a very useful tool for studying dynamical systems. For example, the approach we describe here can be used for designing and planning manufacturing processes such as turning and milling. Specifically, the transition from stable steady state to a limit cycle via a Hopf bifurcation is similar to the transition from stable cutting to unstable cutting where the tool starts to chatter. Therefore, we believe that our approach will have applications in predicting and detecting chatter vibrations in cutting processes. This will allow selecting the cutting parameters so that the process remains chatter-free.

Although the datasets that we investigated were generated using simulation, the developed method is equally applicable to experimental data. Further development of the presented approach is part of the authors' active research.

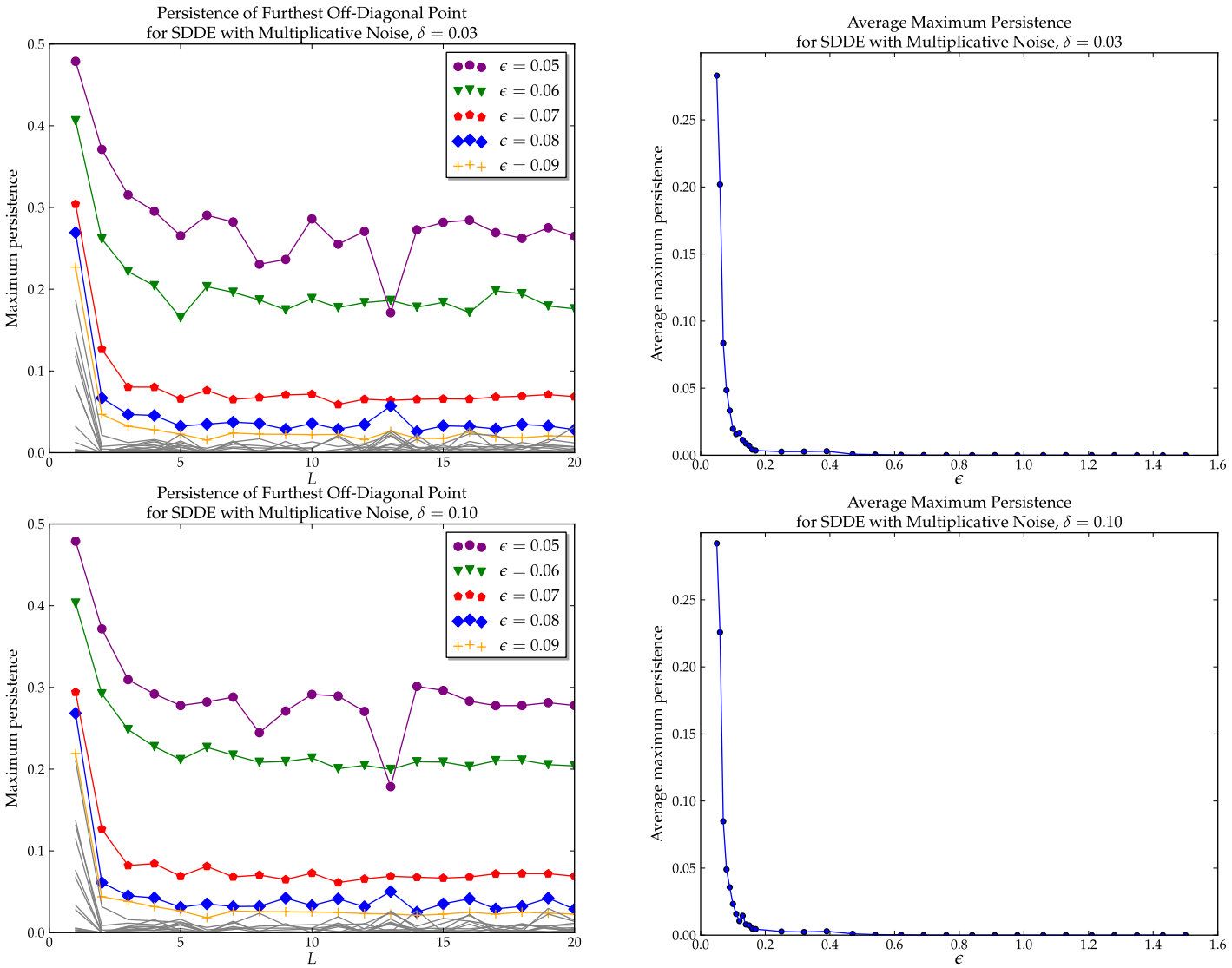

FIGURE 6. Results of analysis of data from simulations using multiplicative noise. The top row corresponds to $\delta = 0.03$ and the bottom row corresponds to $\delta = 0.1$. See the caption of Fig. 5 for a more detailed explanation of graphs.

ACKNOWLEDGMENT

The authors thank Jose Perea for the extremely helpful discussions as well as for providing a Matlab version of the code upon which the authors based their python code.

The work described in this article is a result of a collaboration made possible by the Institute for Mathematics and Its Applications. It was carried out while EAM was a postdoctoral fellow at the IMA during the annual program on Scientific and Engineering Applications of Algebraic Topology. FAK gratefully acknowledges the support and hospitality provided by the IMA during his visit which took place in February 2014.

REFERENCES

[1] Barrio, M., Burrage, K., Leier, A., and Tian, T., 2006. "Oscillatory regulation of hes1: Discrete stochastic delay modelling and simulation". *PLoS Comput Biol,* ***2***(9), 09, p. e117.

[2] Tian, T., Burrage, K., Burrage, P. M., and Carletti, M., 2007. "Stochastic delay differential equations for genetic regulatory networks". *Journal of Computational and Applied Mathematics,* ***205***(2), pp. 696 – 707. Special issue on evolutionary problems.

[3] Buckwar, E., Kuske, R., L'Esperance, B., and Soo, T., 2006. "Noise-sensitivity in machine tool vibrations". *International Journal of Bifurcation and Chaos,* ***16***(08),

pp. 2407–2416.

[4] Klamecki, B., 2004. "Enhancement of the low-level components of milling vibration signals by stochastic resonance". *Proceedings of the Institution of Mechanical Engineers, Part E: Journal of Process Mechanical Engineering,* ***218***(1), pp. 33–41.

[5] Mackey, M. C., and Nechaeva, I. G., 1995. "Solution moment stability in stochastic differential delay equations". *Phys. Rev. E,* ***52***(4), Oct, pp. 3366–3376.

[6] Guillouzic, S., L'Heureux, I., and Longtin, A., 1999. "Small delay approximation of stochastic delay differential equations". *Phys. Rev. E,* ***59***, Apr, pp. 3970–3982.

[7] Elbeyli, O., Sun, J., and Unal, G., 2005. "A semi-discretization method for delayed stochastic systems". *Communications in Nonlinear Science and Numerical Simulation,* ***10***(1), pp. 85–94.

[8] Frank, T. D., and Beek, P. J., 2001. "Stationary solutions of linear stochastic delay differential equations: Applications to biological systems". *Phys. Rev. E,* ***64***, Jul, p. 021917.

[9] Buckwar, E., 2000. "Introduction to the numerical analysis of stochastic delay differential equations". *Journal of Computational and Applied Mathematics,* ***125***(1-2), pp. 297 – 307. Numerical Analysis 2000. Vol. VI: Ordinary Differential Equations and Integral Equations.

[10] Mao, X., and Sabanis, S., 2003. "Numerical solutions of stochastic differential delay equations under local lipschitz condition". *Journal of Computational and Applied Mathematics,* ***151***(1), pp. 215 – 227.

[11] Yuan, C., and Glover, W., 2006. "Approximate solutions of stochastic differential delay equations with markovian switching". *Journal of Computational and Applied Mathematics,* ***194***(2), pp. 207 – 226.

[12] Buckwar, E., and Winkler, R., 2007. "Multi-step maruyama methods for stochastic delay differential equations". *Stochastic Analysis and Applications,* ***25***(5), pp. 933–959.

[13] Hu, Y., Mohammed, S.-E. A., and Yan, F., 2004. "Discrete-time approximations of stochastic delay equations: The milstein scheme". *Annals of Probability,* ***32***(1A), pp. 265–314.

[14] Baker, C. T. H., and Buckwar, E., 2005. "Exponential stability in p-th mean of solutions, and of convergent euler-type solutions, of stochastic delay differential equations". *J. Comput. Appl. Math.,* ***184***(2), Dec., pp. 404–427.

[15] Luo, J., 2007. "A note on exponential stability in pth mean of solutions of stochastic delay differential equations". *Journal of Computational and Applied Mathematics,* ***198***(1), pp. 143 – 148.

[16] Mao, X., 2007. "Exponential stability of equidistant euler-maruyama approximations of stochastic differential delay equations". *Journal of Computational and Applied Mathematics,* ***200***(1), pp. 297 – 316.

[17] Jolliffe, I., 2005. *Principal Component Analysis*. John Wiley & Sons, Ltd.

[18] Abdi, H., and Williams, L. J., 2010. "Principal component analysis". *Wiley Interdisciplinary Reviews: Computational Statistics,* ***2***(4), pp. 433–459.

[19] Borg, I., and Groenen, P. J. F., 2005. *Modern Multidimensional Scaling: Theory and Applications*. Springer.

[20] Roweis, S., and Saul, L., 2000. "Nonlinear dimensionality reduction by locally linear embedding". *Science,* ***290***(5500), p. 23232326.

[21] Belkin, M., and Niyogi, P., 2003. "Laplacian eigenmaps for dimensionality reduction and data representation". *Neural Computation,* ***15***(6), pp. 1373–1396.

[22] Donoho, D. L., and Grimes, C., 2003. "Hessian eigenmaps: Locally linear embedding techniques for high-dimensional data". *Proceedings of the National Academy of Sciences,* ***100***(10), pp. 5591–5596.

[23] Zhang, Z., and Zha, H., 2002. "Principal manifolds and nonlinear dimension reduction via local tangent space alignment". *SIAM Journal of Scientific Computing,* ***26***, pp. 313–338.

[24] Coifman, R. R., and Lafon, S., 2006. "Diffusion maps". *Applied and Computational Harmonic Analysis,* ***21***(1), pp. 5 – 30. Special Issue: Diffusion Maps and Wavelets.

[25] Nadler, B., Lafon, S., Coifman, R. R., and Kevrekidis, I. G., 2006. "Diffusion maps, spectral clustering and reaction coordinates of dynamical systems". *Applied and Computational Harmonic Analysis,* ***21***(1), pp. 113 – 127. Special Issue: Diffusion Maps and Wavelets.

[26] Singer, A., and Coifman, R. R., 2008. "Non-linear independent component analysis with diffusion maps". *Applied and Computational Harmonic Analysis,* ***25***(2), pp. 226 – 239.

[27] Klosek, M., and Kuske, R., 2005. "Multiscale analysis of stochastic delay differential equations". *Multiscale Modeling & Simulation,* ***3***(3), pp. 706–729.

[28] Kim, S., Park, S. H., and Pyo, H.-B., 1999. "Stochastic resonance in coupled oscillator systems with time delay". *Phys. Rev. Lett.,* ***82***, Feb, pp. 1620–1623.

[29] Ohira, T., and Sato, Y., 1999. "Resonance with noise and delay". *Phys. Rev. Lett.,* ***82***, Apr, pp. 2811–2815.

[30] Masoller, C., 2002. "Noise-induced resonance in delayed feedback systems". *Phys. Rev. Lett.,* ***88***(3), p. 34102.

[31] Kuske, R., 2006. "Multiple-scales approximation of a coherence resonance route to chatter". *Computing in Science Engineering,* ***8***(3), pp. 35–43.

[32] Kuske, R., 2010. "Competition of noise sources in systems with delay: The role of multiple time scales". *Journal of Vibration and Control,* ***16***(7-8), pp. 983–1003.

[33] Luo, X., Wu, D., and Zhu, S., 2012. "Stochastic resonance in a time-delayed bistable system with colored coupling between noise terms". *International Journal of Modern*

Physics B, ***26***(30), p. 1250149.

[34] Brown, J., and Gedeon, T., 2012. "Structure of the afferent terminals in terminal ganglion of a cricket and persistent homology". *PLoS ONE,* ***7***(5), 05, p. e37278.

[35] Nicolau, M., Levine, A. J., and Carlsson, G., 2011. "Topology based data analysis identifies a subgroup of breast cancers with a unique mutational profile and excellent survival". *Proceedings of the National Academy of Sciences,* ***108***(17), pp. 7265–7270.

[36] de Silva, V., and Ghrist, R., 2007. "Coverage in sensor networks via persistent homology". *Algebraic & Geometric Topology,* ***7***, Apr., pp. 339–358.

[37] Munch, E., Shapiro, M., and Harer, J., 2012. "Failure filtrations for fenced sensor networks". *The International Journal of Robotics Research,* ***31***(9), pp. 1044–1056.

[38] Carlsson, G., Ishkhanov, T., de Silva, V., and Zomorodian, A., 2008. "On the local behavior of spaces of natural images". *International Journal of Computer Vision,* ***76***, pp. 1–12. 10.1007/s11263-007-0056-x.

[39] Munkres, J. R., 1993. *Elements of Algebraic Topology*. Addison Wesley.

[40] Hatcher, A., 2002. *Algebraic Topology*. Cambridge University Press.

[41] Edelsbrunner, H., and Harer, J., 2010. *Computational Topology: An Introduction*. American Mathematical Society.

[42] Edelsbrunner, H., Letscher, D., and Zomorodian, A., 2000. "Topological persistence and simplification". In Foundations of Computer Science, 2000. Proceedings. 41st Annual Symposium on, pp. 454 –463.

[43] Perea, J., and Harer, J., 2013. "Sliding windows and persistence: An application of topological methods to signal analysis". *arXiv:1307.6188*.

[44] Berwald, J., Gidea, M., and Vejdemo-Johansson, M., 2013. "Automatic recognition and tagging of topologically different regimes in dynamical systems". *arXiv:1312.2482*.

[45] Higham, D., 2001. "An algorithmic introduction to numerical simulation of stochastic differential equations". *SIAM Review,* ***43***(3), pp. 525–546.

[46] Harer, J., Slaczedek, J., and Bendich, P., 2014. "Ripscollapse: discrete morse theory and fast computation of one-dimensional persistence.". *Manuscript, Duke University*.